

Supporting Information

Noncovalent Backbone Planarization Strategy Increase NIR-II Extinction Coefficients for Gas/Phototheranostic Applications

Peng Cheng^{a#}, Shangyu Chen^{a##}, Jiwei Li^b, Wan Yang^a, Pengfei Chen^a, Han Miao^c, Qingming Shen^a, Pengfei Sun^{a}, and Quli Fan^{a*}*

^aState Key Laboratory of Organic Electronics and Information Displays & Institute of Advanced Materials (IAM), Nanjing University of Posts & Telecommunications, Nanjing 210023, China

^bKey Laboratory of Flexible Electronics (KLOFE) & Institute of Advanced Materials (IAM), Jiangsu National Synergetic Innovation Center for Advanced Materials (SICAM), Nanjing Tech University (NanjingTech), Nanjing 211816, China

^cSchool of Materials Science and Engineering, East China University of Science and Technology, Shanghai 200237, China

Corresponding authors (emails: 18260038928@163.com (Chen S); iampfsun@njupt.edu.cn (Sun P); iamqlfan@njupt.edu.cn (Fan Q))

1. General information and methods

1.1. Materials. All original donor and acceptor used in subsequent experiments were purchased from SunaTech Inc. Catalyst tetrakis(triphenylphosphine)palladium ($\text{Pd}(\text{PPh}_3)_4$) and S-Nitroso-N-acetyl-DL-penicillamine (SNAP) were obtained from J&K Scientific Ltd. N-azidoacetylmannosamine-tetraacylated (Ac4ManNAz), and 1,2-distearoyl-sn-glycero-3-phosphoethanolamine-N[methoxy-(poly(ethylene glycol))-2000] (DSPE-PEG_{2K}) were purchased from Sigma-Aldrich Chemical Co. Dulbecco's modified eagle medium (DMEM), fetal bovine serum (FBS), Annexin V-FITC/propidium iodide (PI) cell apoptosis kit, calcein-AM/propidium iodide (PI) cell apoptosis kit, 3-amino-4-aminomethyl-2',7'-difluorescein, diacetate (DAF-FM DA), and the Griess reagent kit were purchased from KeyGEN BioTECH.

1.2. Characterization. All ^1H NMR spectra of the synthesized conjugated small molecules (CSMs) were conducted by a Bruker Ultra Shield Plus NMR instrument (400 MHz). Tetramethylsilane (TMS) was selected as the internal standard with CDCl_3 as the deuterated solvent. MALDI-TOF spectra was recorded through a Bruker autoflex speed MALDI-TOF instrument with cyano-4-hydroxycinnamic acid in CHCl_3 as the matrix. TEM images were obtained from a HT7700 transmission electron microscope (100 KV). DLS analysis was characterized by a commercial laser light scattering spectrometer (ALV-7004, Langen, Germany), which is equipped with a multi- τ digital time correlator as well as a He-Ne laser (at $\lambda = 632.8$ nm). The test was conducted with 90° scattering angle at room temperature. Shimadzu UV-3600 spectrophotometer and NIR-II spectrophotometer (Fluorolog 3, Horiba) were used to record the absorption and

fluorescence emission spectra. The 808 nm and 1064 nm diode laser we used were purchased from Changchun New Industries Optoelectronics Technology Co., Ltd. Cell imaging was conducted by Confocal Laser Scanning Microscopy (CLSM, Olympus Fluoview FV1000). NIR-II fluorescence imaging experiments was conducted on an NIR-II imaging system (Wuhan Grand-imaging Technology Co., Ltd). A 640×512 pixel two-dimensional InGaAs array from Princeton Instruments in NIR-II fluorescence windows was equipped in this NIR-II fluorescence imaging system. A Fluke TI400 thermal imaging camera was used to monitor the temperature changes under light irradiation.

1.3. General preparation of B-Xs NPs. DSPE-PEG_{2K} (20 mg) and CSMs (1.0 mg) (mass ratio = 20 : 1) were dissolved in water (10 mL) and tetrahydrofuran (THF, 1.0 mL), respectively. The THF solution was dropwise added into water with a volume ratio 0.1 in an ultrasonic vibrator (100 Hz). Then, pure nitrogen was bubbled through the solution to remove THF. The rest NPs aqueous solution was evaporated or diluted to a required concentration.

1.4. NIR-II photothermal performance test. The aqueous solutions of all NPs with a specified concentration (100 μ M) were prepared and sealed into plastic tubes to examine the photothermal performance in presence of 1064 nm laser irradiation (1.0 W cm^{-2} , 5 min). Using a Fluke TI400 thermal imaging camera, the temperature was measured every 30 s and stopped until the temperature nearly reached to a plateau, and the corresponding thermal images were real-timely acquired as well. In addition, the NIR-II photothermal conversion efficiency (PCE, η) of NPs was calculated according

to the literature.^[1]

1.5. *In vitro NO release.* The NO release was detected by Griess reagent in vitro. Griess reagent was dissolved completely in water and added to B-E-NO NPs aqueous solution. Then, the mixed solution was immediately transferred into a UV quartz cuvette with a lid. After 1064 nm laser irradiation for a period, the UV absorption of the solution at 540 nm was measured using UV spectrophotometer.

1.6. *Intracellular NO detection by confocal imaging and flow cytometry.* The intracellular NO was detected using a NO probe (DAF-FM DA). 4T1 cells were inoculated in a cell culture dish and incubated with complete DMEM (containing 10% FBS) for 24 h under standard condition (37 °C, 5% CO₂) in dark. Then, B-E-NO NPs were added to fresh DMEM. After co-incubation with the mixed medium for 2 h in the dark, the cells were irradiated with a 1064 nm laser (1.0 W cm⁻²) for 5 min. Then, the medium was removed, and the cells were stained with 1.0 mL of fresh DMEM. After that, the cells were moved to standard conditions (37 °C, 5% CO₂) for 20 min, followed by incubating with DAF-FM DA working solution at 37 °C for 20 min. Cells were washed twice with PBS buffer, and then 1.0 mL of fresh DMEM was added to the cells. Finally, the cells were imaged by CLSM. In addition, NO detection was also confirmed by flow cytometry.

1.7. *In vitro mitochondrial membrane potential (JC-1 test).* 4T1 cells were inoculated in a cell culture dish and incubated with complete DMEM (containing 10% FBS) for 24 h under standard condition (37 °C, 5% CO₂) in dark. Then, B-E-NO NPs were added to fresh DMEM to obtain the mixed medium (100 μM). After co-incubation with the

mixed medium for 4 h in the dark, the media were removed and the cells were stained with 1.0 mL fresh DMEM. After 5 min irradiation of 1064 nm laser at a power of 1.0 W cm⁻², three dishes were removed to the standard condition (37 °C, 5% CO₂) for 6 h to allow cells to undergo apoptosis. Then, cells were incubated with JC-1 working solution for 20 min at 37 °C. The cells were washed twice with IX Incubation Buffer and 1.0 mL fresh DMEM was added to the cells. The fluorescence of JC-1 of cells with or without 1064 nm laser irradiation and click treatment were observed by CLSM (Olympus Fluoview FV1000).

1.8. Assessment of *in vitro* NIR-II excitation PTT and NO synergistic therapies by confocal imaging assay. 4T1 cells were cultured with DMEM in CLSM culture dishes (Costar) until the cell density increased to 1×10⁵ cells mL⁻¹ per well. Materials in different groups were added to fresh DMEM to obtain the mixed medium (100 μM). After the 4T1 cells had been co-incubated with this mixed medium for 4 h in the dark, the media were removed, the cells were washed by PBS and replaced with fresh DMEM. Next, the selected wells from different groups were illuminated with or without a 1064 nm laser at a power of 1.0 W cm⁻² for 5 min. After a 24 h incubation to allow cells to undergo apoptosis, the medium was removed and the cells were incubated with Calcein AM/propidium iodide (PI) solution for 30 min. Next, the cells were washed by PBS and replaced with 1.0 mL fresh DMEM. Then, the cells were imaged by CLSM (Olympus Fluoview FV1000).

1.9. Assessment of *in vitro* NIR-II excitation PTT and NO synergistic therapies using flow cytometry assay. 4T1 cells were cultured with DMEM in 6-well plates until the

cell density increased to 1.0×10^5 cells mL^{-1} per well. Materials in different groups were added to fresh DMEM to obtain the mixed medium (100 μM). After the 4T1 cells had been co-incubated with this mixed medium for 4 h in the dark, the media were removed and replaced with 1.0 mL fresh DMEM. Next, the selected wells from different groups were illuminated with or without a 1064 nm laser at a power of 1.0 W cm^{-2} for 5 min. After a 24 h incubation to allow cells to undergo apoptosis, the 4T1 cells that had detached from the 6-well plates were washed several times with 1.0 mL PBS. Subsequently, PBS was removed and 500 μL trypsin digestion solution without EDTA was added, and the cells were dissolved in an incubator at $37 \text{ }^\circ\text{C}$ and 5% CO_2 for 90 s. Later 1.0 mL of DMEM was added and the cells were transferred into a 15 mL centrifuge tube and centrifuged for 3 min. An Annexin V-FITC/PI staining solution was then mixed with the collected cells for 15 min, and cells were analyzed using flow cytometry.

1.10. *In vivo NIR-II light excited NIR-II FLI and NIR-II PAI.* Before imaging experiments, the hair of mice in the interested section were removed by commercial hair removal cream gel. Then the mice were administered with B-E-NO NPs at a concentration of 2 mg mL^{-1} (150 μL) via tail vein. For tumor imaging, the whole body of mice were imaged at different time points after injection. Meanwhile, the *in vivo* NIR-II PAI was also carried out on a TomoWave3D, Medical Imaging Co., Ltd., at designated time intervals after injection of B-E-NO NPs.

1.11. *In vivo NIR-II excitation PTT and NO synergistic therapies.* When tumor volume reached $90\text{-}120 \text{ mm}^3$, all 4T1 tumor-bearing mice were weighed and randomly

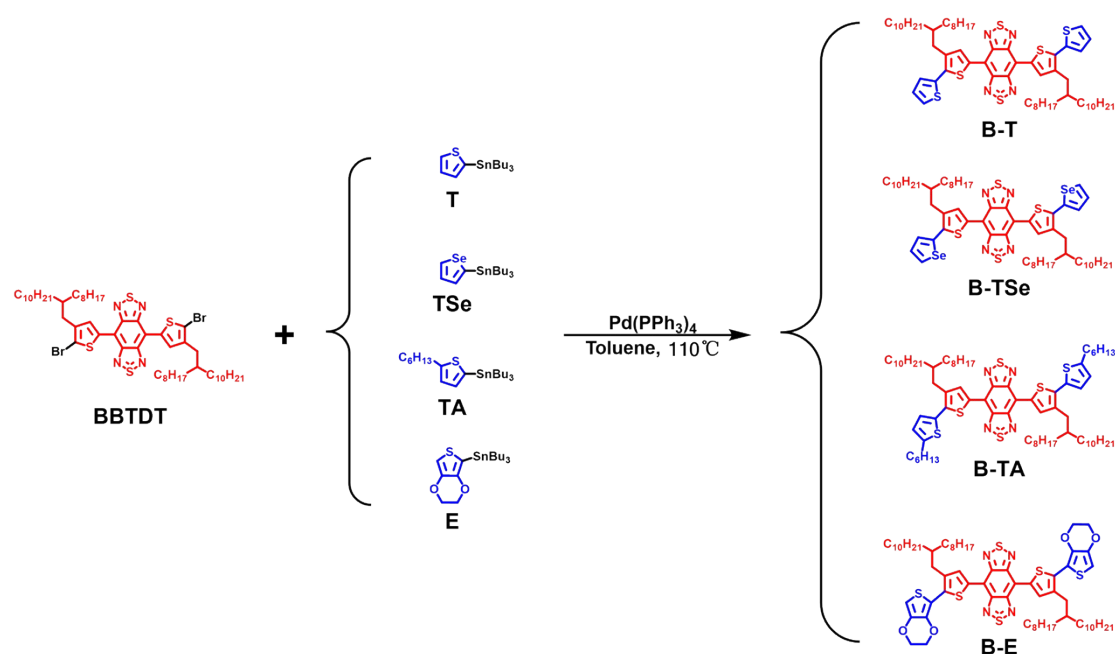
classified into four groups denoted as “PBS”, “B-E-NO NPs”, “B-E NPs + L”, and “B-E-NO NPs + L”, respectively. On day 0, for “PBS” and “B-E-NO NPs” groups, 150 μL of PBS and 150 μL , 2 mg mL^{-1} of B-E-NO NPs were first injected into 4T1 tumor-bearing mice through tail vein without subsequent laser irradiation. In the case of “B-E NPs + L”, and “B-E-NO NPs + L” groups, after intravenous injection 150 μL , 2 mg mL^{-1} of B-E NPs and B-E-NO NPs for 24 h, respectively, the tumor sites were continuously irradiated by 1064 nm laser (1.0 W cm^{-2}) for 5 min. During the therapeutic process, the tumor temperature changes were real-timely monitored and recorded by Fluke TI400 thermal imaging camera.

1.12. Histological analysis. All the mice were sacrificed after complete treatment of 15 days. The major organs (heart, liver, spleen, lung and kidney) were dissected from the mice. After the tissues were fixed in 4% (v/v) formalin overnight, they were embedded in paraffin and sectioned at 5 μm thickness. The sections were then subjected to H&E staining for histopathological evaluation.

1.13. Animal experiments. All small animal experiments were carried out in accordance with the specifications of The National Regulation of China for Care and Use of Laboratory Animals, which have been approved by the Jiangsu Administration of Experimental Animals. Five- or six-week-old BALB/c mice were purchased from KeyGEN BioTECH. Co., Ltd (Nanjing, China) with pathogen-free feeding environment, whose accreditation numbers are SYXK 2017-0040 and SCXK 2017-0005, respectively. The xenograft tumor models were established by subcutaneous injection of 1.0×10^6 4T1 cells into the right flanks of each mouse.

1.12. Statistical analysis. Unless otherwise stated, statistical comparisons between various groups were performed using with one-way analysis of variance (ANOVA) with a corrected p value below 0.05 considered statistically to be significant (*p < 0.05, **p < 0.01, ***p < 0.001). All data were generated from the mean values of three independent experiments and are presented as the mean ± standard deviation (s.d.).

2. Synthetic procedures of compounds



Scheme S1. Synthetic procedures of B-Xs.

(1) Synthetic procedure of B-T. 4,8-Bis(5-bromo-4-(2-octyldodecyl)thiophen-2-yl)-benzo[1,2-c;4,5-c']bis[1,2,5]thiadiazole (BBTDT, 107 mg, 0.1 mmol), tributyl(thiophen-2-yl)stannane (T, 112 mg, 0.3 mmol), and tetrakis(triphenylphosphine)palladium (Pd(PPh₃)₄, 5 mg, 4 μmol) were both dissolved in dry toluene (3 mL) under N₂ protection. After refluxing for 12 h at 110 °C in dark and then cooling to room temperature, the mixture was poured into water and extracted twice with dichloromethane (DCM)/water. The organic phase was dried with

anhydrous sodium sulfate and evaporated via vacuum treatment. The crude product was subjected to column chromatography on silica gel with PE/DCM 7:3 as eluent to afford B-T (90 mg, 83%). ¹H NMR (400 MHz, CDCl₃, ppm) δ: 8.85 (s, 2H), 7.17-7.16 (d, 2H), 6.80-6.79 (d, 2H), 2.88-2.84 (t, 8H), 1.26-1.22 (m, 62H), 0.86-0.84 (m, 14H). ¹³C NMR (100 MHz, CDCl₃, ppm) δ: 151.28, 147.00, 139.12, 138.13, 136.73, 135.11, 133.76, 126.16, 124.67, 112.78, 38.63, 33.95, 33.48, 31.95, 31.63, 30.28, 30.16, 29.78, 29.40, 28.89, 26.51, 22.71, 14.15.

(2) Synthetic procedure of B-TSe. For the synthesis of B-TSe, the reaction conditions were fixed the same like that of B-T except the donor unit. Changing T to tributyl(selenophen-2-yl)stannane (TSe, 126 mg, 0.3 mmol), the final crude product was purified by column chromatography with PE/DCM 3:1 as eluent to afford B-TSe (98 mg, 84%). ¹H NMR (400 MHz, CDCl₃, ppm) δ: 8.84 (s, 2H), 8.37-8.35 (d, 1H), 8.09-8.07 (d, 2H), 7.87-7.86 (d, 1H), 7.70-7.64 (m, 2H), 7.55-7.44 (m, 8H), 7.38-7.35 (d, 2H), 7.23-7.21 (d, 1H), 2.86-2.84 (d, 4H), 1.24-1.21 (m, 42H), 0.92-0.90 (m, 25H). ¹³C NMR (100 MHz, CDCl₃, ppm) δ: 151.07, 141.12, 139.81, 139.39, 137.92, 135.50, 135.32, 132.17, 131.63, 130.57, 130.05, 129.69, 128.59, 128.57, 112.64, 38.71, 34.02, 33.46, 31.96, 30.18, 29.79, 29.41, 28.99, 27.88, 27.31, 27.02, 26.49, 22.72, 14.16, 13.67, 11.13.

(3) Synthetic procedure of B-TA. For the synthesis of B-TA, the reaction conditions were fixed the same like that of B-T except the donor unit. Changing T to tributyl(5-hexylthiophen-2-yl)stannane (TA, 127 mg, 0.3 mmol), the final crude product was purified by column chromatography with PE/DCM 1:1 as eluent to afford B-TA (108

mg, 86%). ^1H NMR (400 MHz, CDCl_3 , ppm) δ : 8.85 (s, 2H), 7.17-7.16 (d, 2H), 6.79-6.78 (d, 2H), 2.87-2.83 (t, 8H), 1.77-1.69 (m, 4H), 1.35-1.21 (m, 76H), 0.93-0.82 (m, 20H). ^{13}C NMR (100 MHz, CDCl_3 , ppm) δ : 151.23, 146.96, 139.08, 138.10, 136.71, 135.08, 133.75, 126.14, 124.65, 112.73, 38.62, 33.94, 33.47, 31.97, 31.63, 30.27, 30.16, 29.78, 29.40, 28.89, 26.49, 22.71, 14.15.

(4) Synthetic procedure of B-E. For the synthesis of B-E, the reaction conditions were fixed the same like that of B-T except the donor unit. Changing T to tributyl(2,3-dihydrothieno[3,4-*b*][1,4]dioxin-5-yl)stannane (E, 130 mg, 0.3 mmol), the final crude product was purified by column chromatography with PE/DCM 2:1 as eluent to afford B-E (98 mg, 82%). ^1H NMR (400 MHz, CDCl_3 , ppm) δ : 8.88 (s, 2H), 6.45 (s, 2H), 4.38-4.27 (m, 8H), 2.85-2.83 (d, 4H), 1.32-1.22 (d, 66H), 0.87-0.82 (m, 12H), ^{13}C NMR (100 MHz, CDCl_3 , ppm) δ : 151.32, 141.64, 140.89, 138.65, 136.57, 136.09, 134.49, 112.96, 111.00, 99.73, 65.02, 64.54, 38.66, 34.11, 33.46, 31.94, 30.16, 29.71, 29.39, 26.53, 22.71, 14.15.

3. Supplementary tables and figures

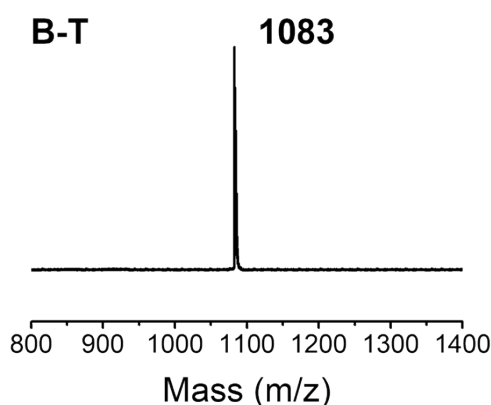


Fig. S1. MALDI-TOF mass spectrometry of B-T.

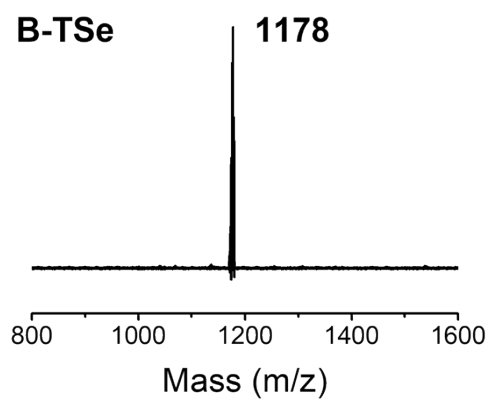


Fig. S2. MALDI-TOF mass spectrometry of B-TSe.

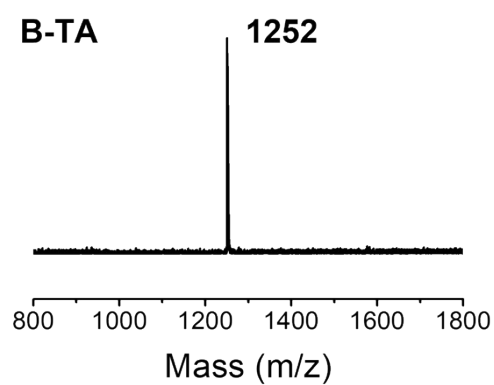


Fig. S3. MALDI-TOF mass spectrometry of B-TA.

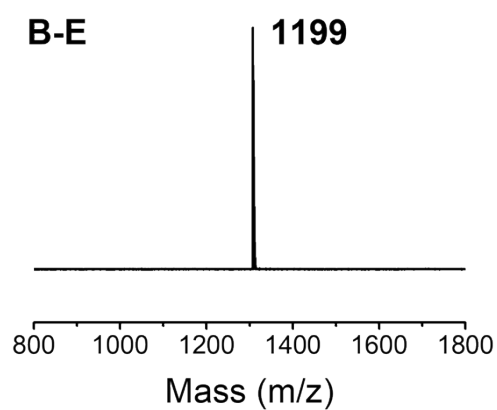


Fig. S4. MALDI-TOF mass spectrometry of B-E.

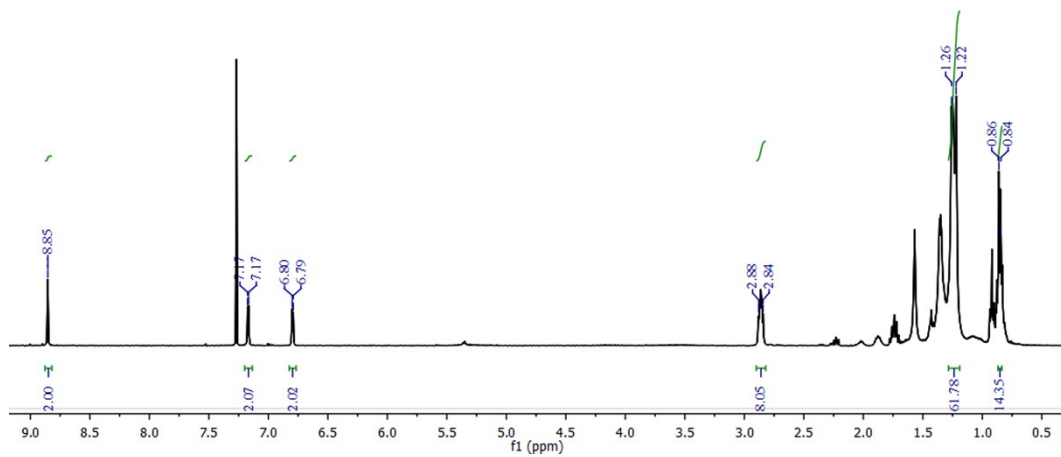
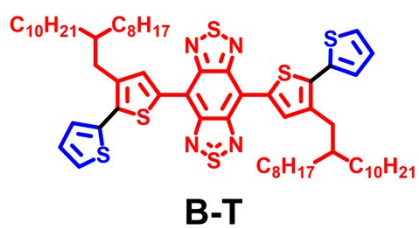


Fig. S5. ^1H NMR spectra of B-T in CDCl_3 .

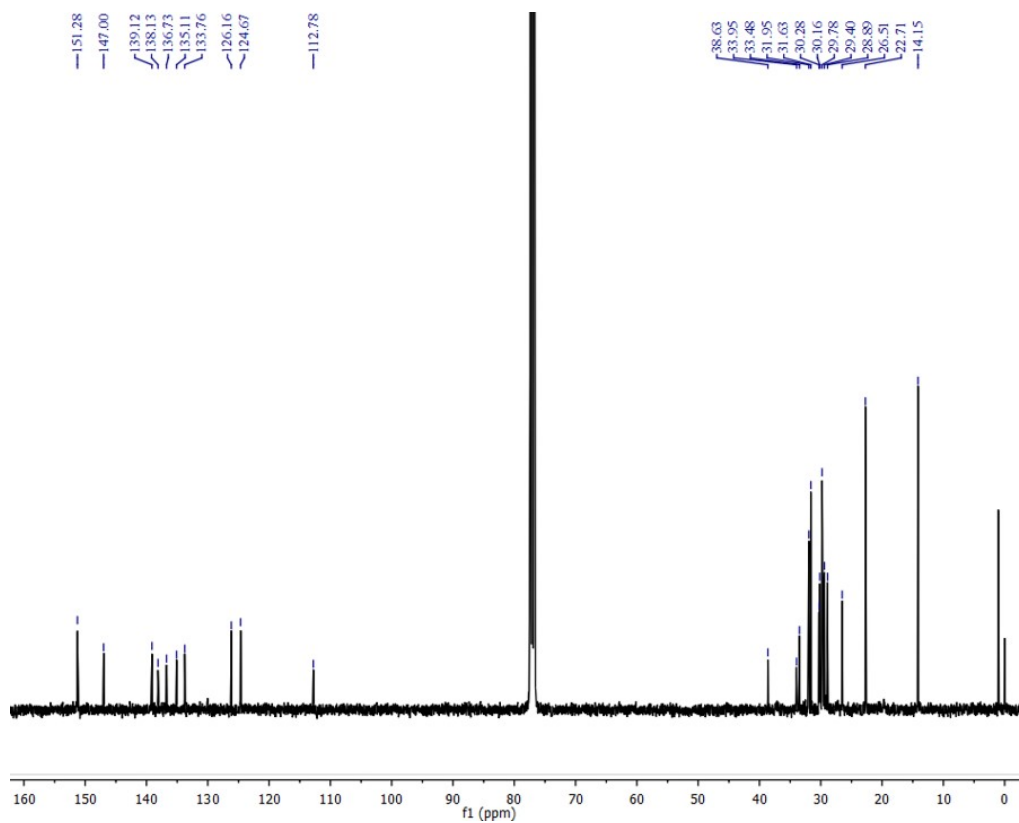


Fig. S6. ^{13}C NMR spectra of B-T in CDCl_3 .

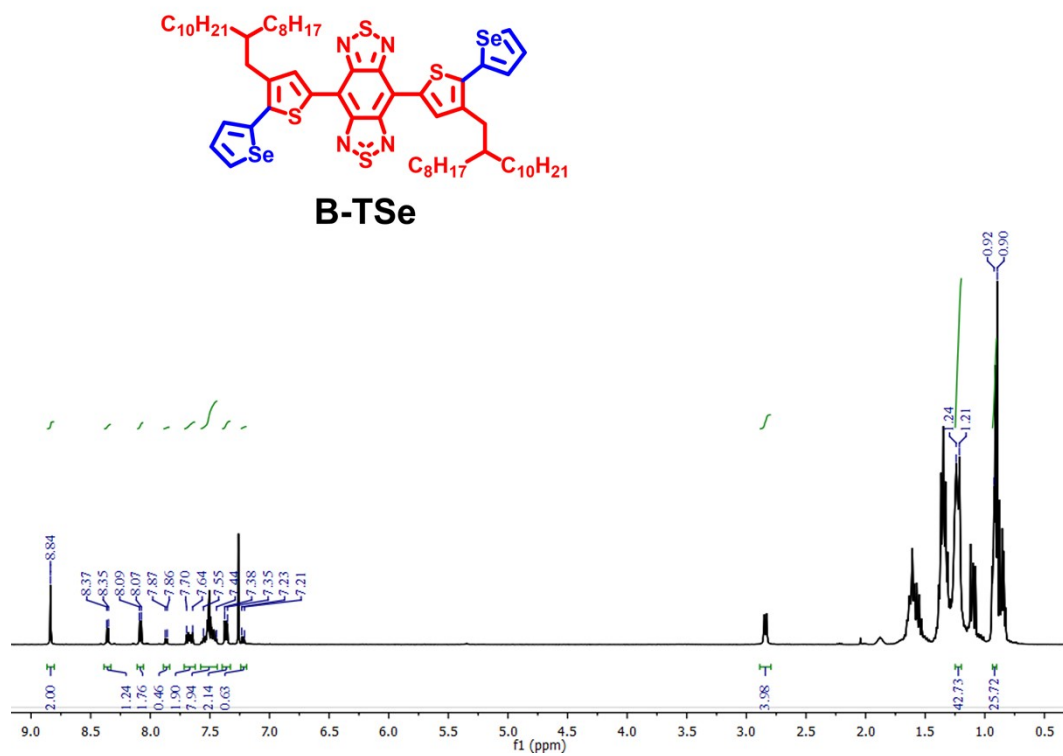


Fig. S7. ^1H NMR spectra of B-TSe in CDCl_3 .

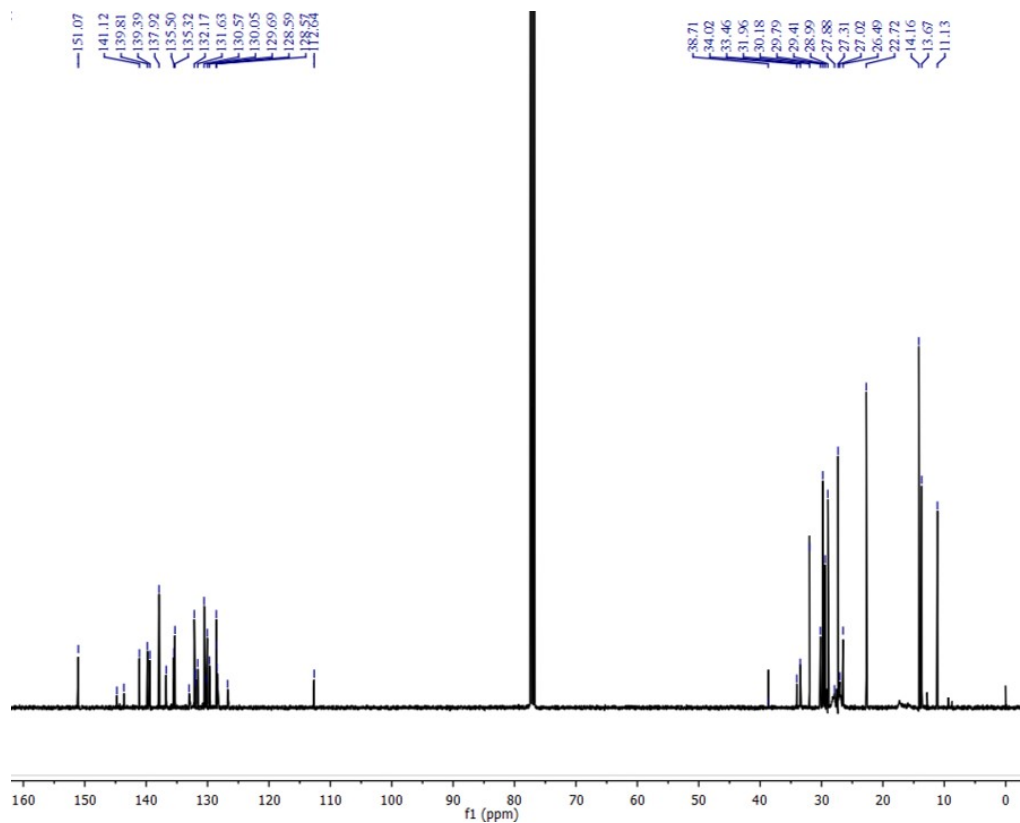


Fig. S8. ^{13}C NMR spectra of B-TSe in CDCl_3 .

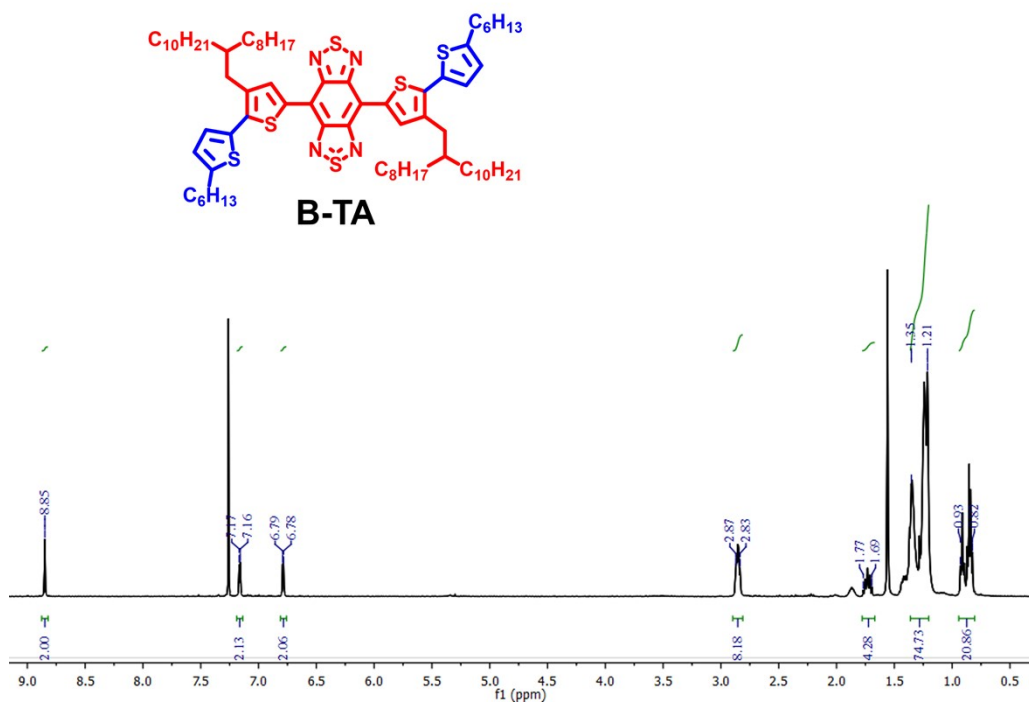


Fig. S9. ^1H NMR spectra of B-TA in CDCl_3 .

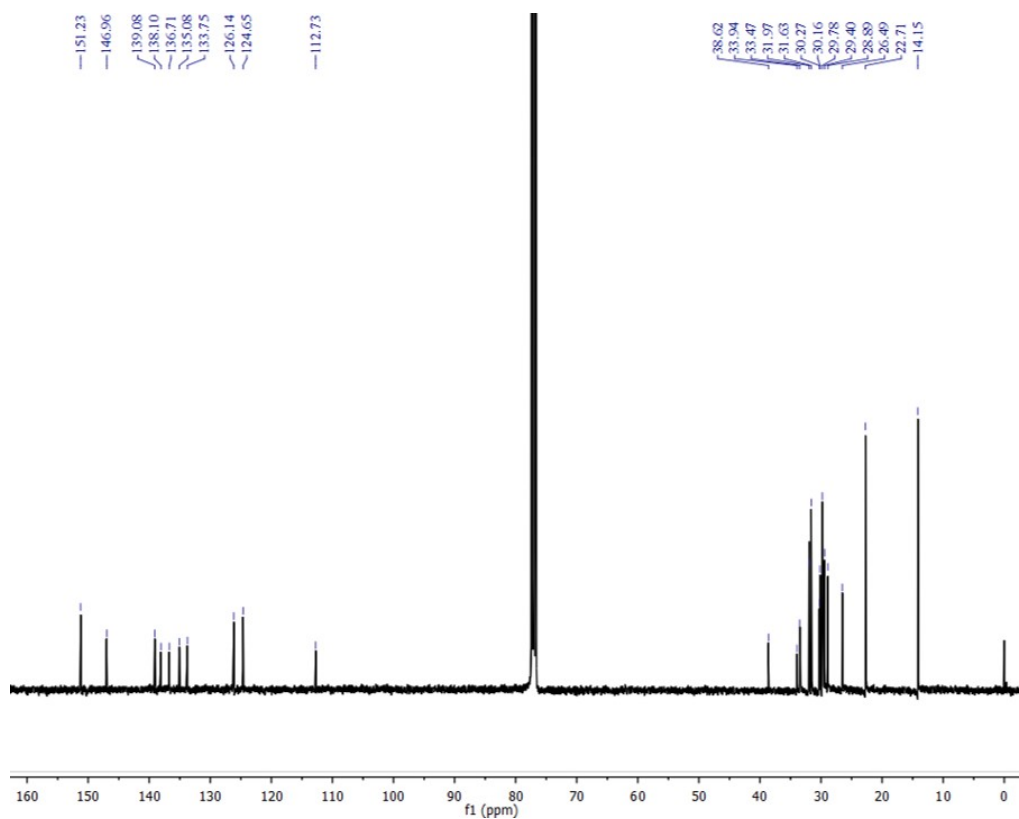


Fig. S10. ^{13}C NMR spectra of B-TA in CDCl_3 .

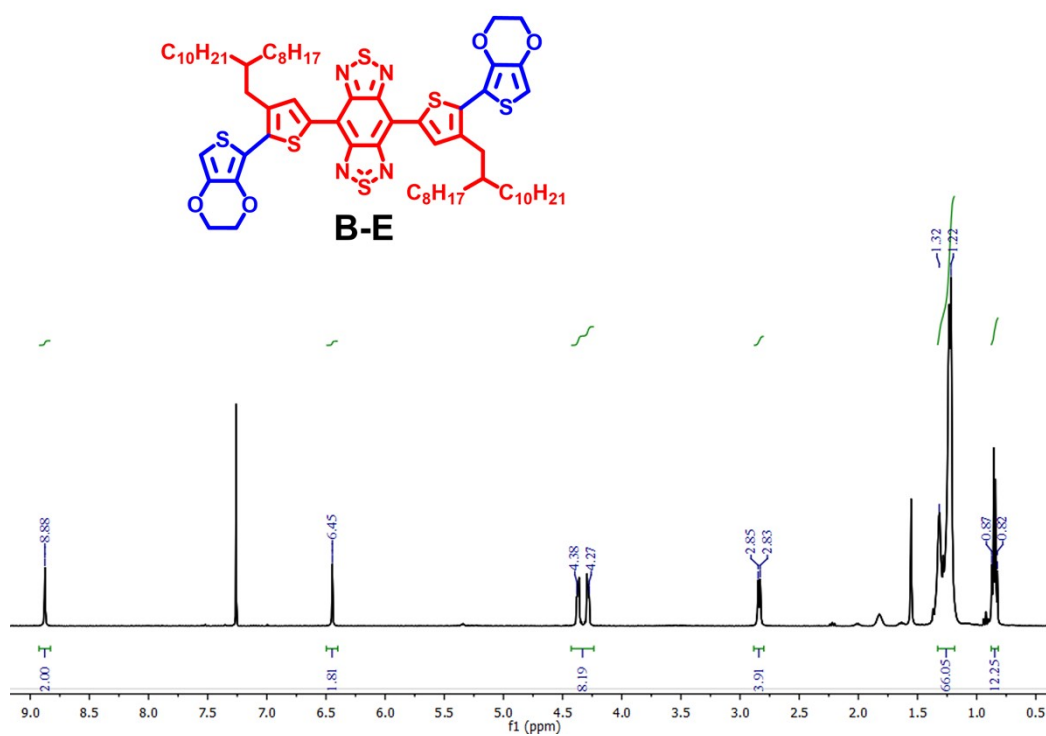


Fig. S11. ^1H NMR spectra of B-E in CDCl_3 .

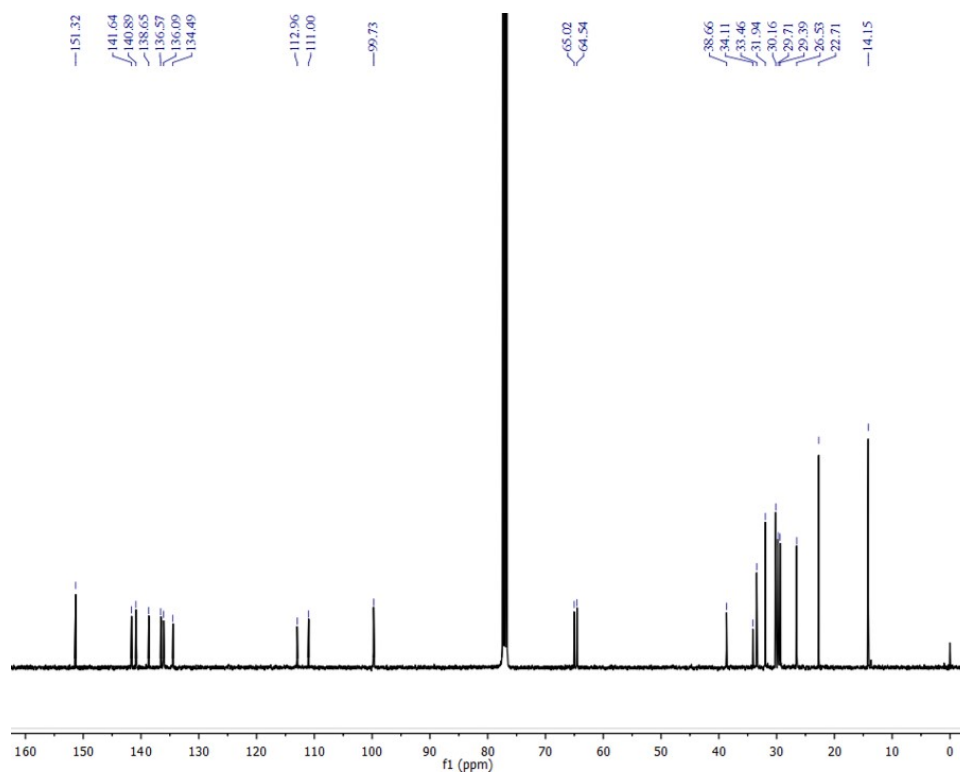


Fig. S12. ^{13}C NMR spectra of B-E in CDCl_3 .

Table S1. Optical data of NIR-II fluorophores.

Samples	λ_{abs} [nm]	λ_{em} [nm]	Stoke shift [nm]	ϵ_{1064} [$10^3 \text{ M}^{-1} \text{ cm}^{-1}$]
B-T ^{a)}	800	1045	245	0.024
B-T NPs ^{b)}	811	1074	263	0.51
B-TSe ^{a)}	817	1062	245	0.16
B-TSe NPs ^{b)}	831	1086	255	0.81
B-TA ^{a)}	831	1052	221	0.21
B-TA NPs ^{b)}	853	1115	262	2.24
B-E ^{a)}	834	1094	260	0.63
B-E NPs ^{b)}	1003	1109	106	10.0

^{a)}Data measured in THF; ^{b)}Data measured in water.

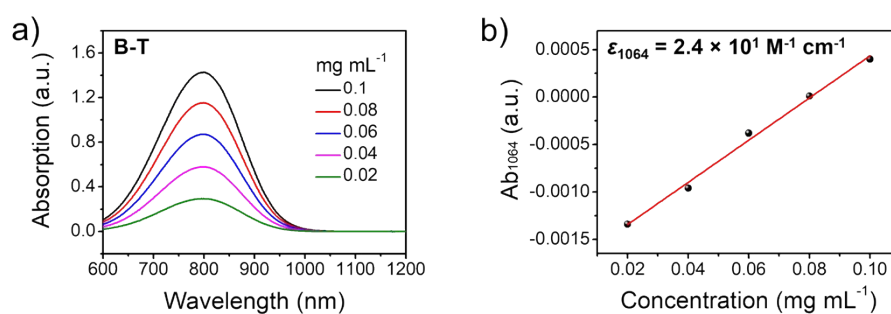


Fig. S13. (a) UV-vis-NIR spectra of B-T in THF at different concentration. (b) The mole extinction coefficient of B-T at 1064 nm.

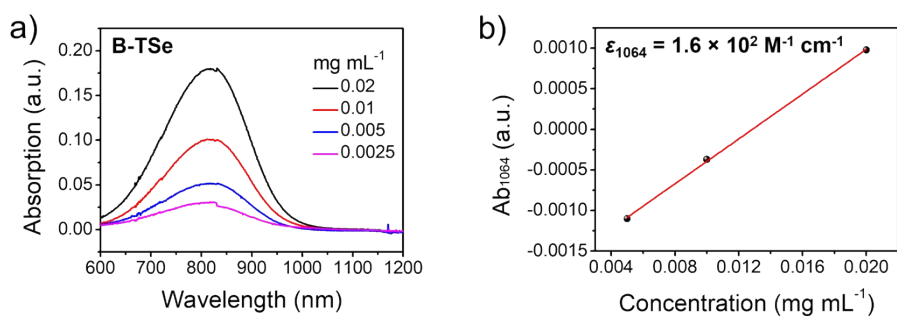


Fig. S14. (a) UV-vis-NIR spectra of B-TSe in THF at different concentration. (b) The mole extinction coefficient of B-TSe at 1064 nm.

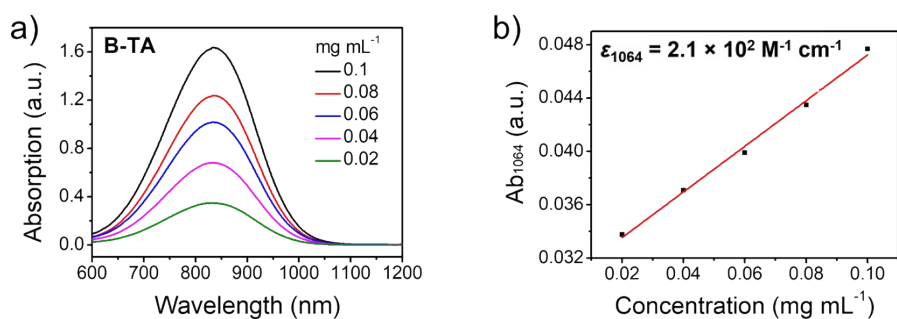


Fig. S15. (a) UV-vis-NIR spectra of B-TA in THF at different concentration. (b) The mole extinction coefficient of B-TA at 1064 nm.

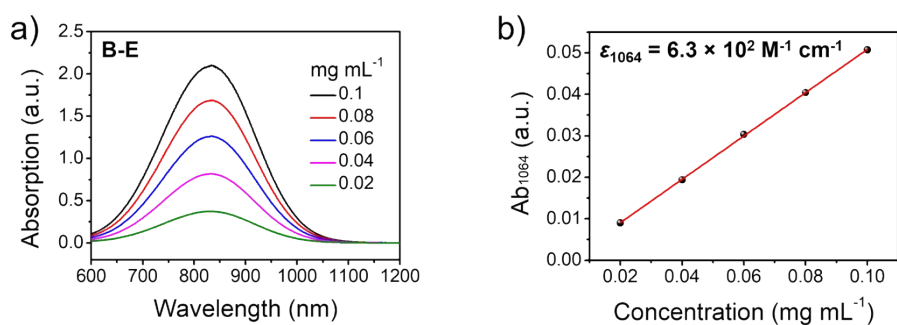


Fig. S16. (a) UV-vis-NIR spectra of B-E in THF at different concentration. (b) The mole extinction coefficient of B-E at 1064 nm.

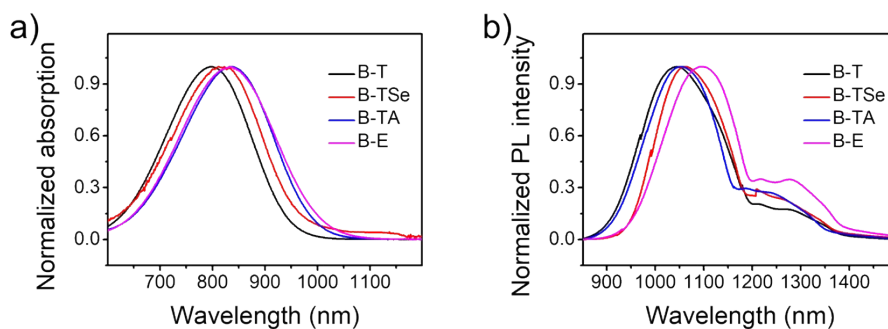


Fig. S17. (a) Normalized absorption and (b) NIR-II fluorescence emission spectra (excited by 808 nm laser) of B-Xs in THF at the same concentration (100 μ M).

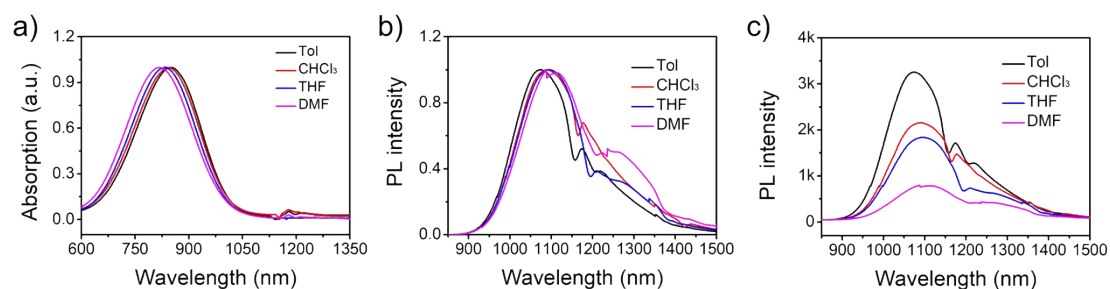


Fig. 18. (a) Normalized absorption spectra and (b) normalized NIR-II fluorescence emission spectra of B-E in different solvents. (c) The NIR-II fluorescence emission spectra of B-E in different solvents under the same concentration of 100 μ M. B-E exhibited a negligible peak variation in absorption and a significant intensity decrease in fluorescence emission with an increase in solvent polarity, which indicates twisted intramolecular charge transfer in large polar solvents, favoring its NIR-II absorption/emission.

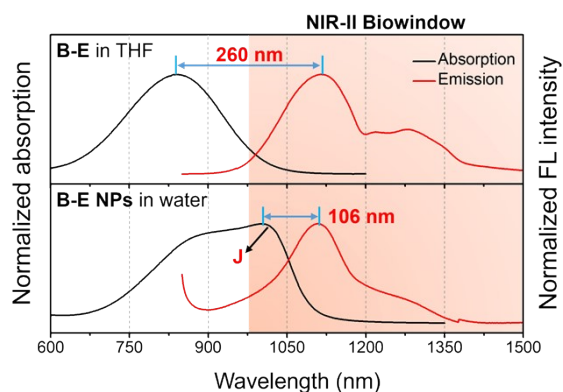


Fig. S19. Normalized absorption (left, black) and emission (right, red) spectra of B-E in THF and B-E NPs in water.

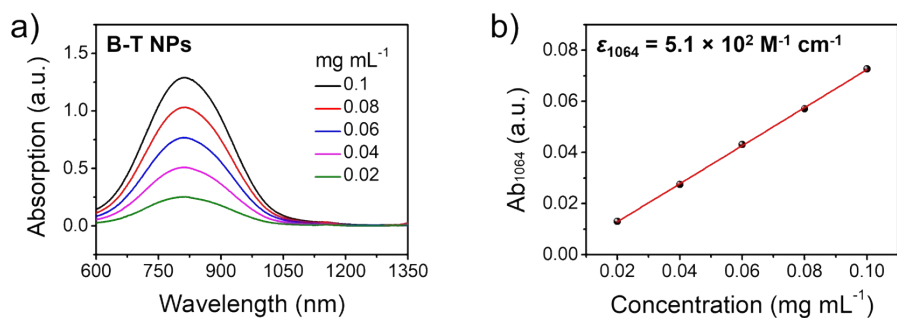


Fig. S20. (a) UV-vis-NIR spectra of B-T NPs in water at different concentration. (b)

The mole extinction coefficient of B-T NPs at 1064 nm.

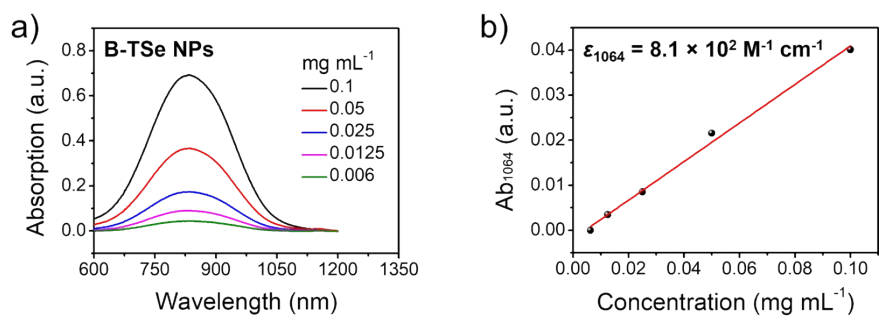


Fig. S21. (a) UV-vis-NIR spectra of B-TSe NPs in water at different concentration. (b)

The mole extinction coefficient of B-TSe NPs at 1064 nm.

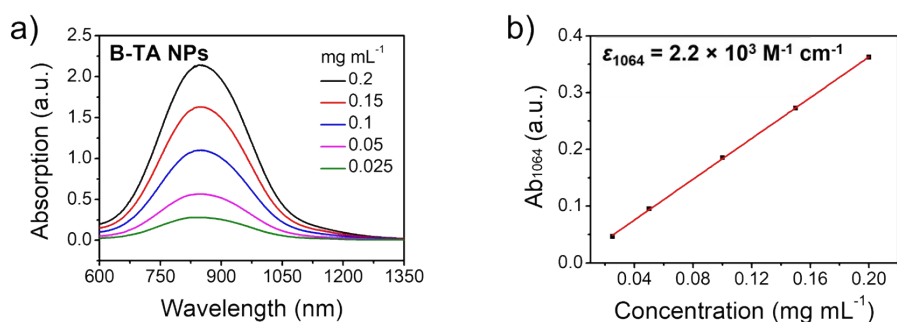


Fig. S22. (a) UV-vis-NIR spectra of B-TA NPs in water at different concentration. (b)

The mole extinction coefficient of B-TA NPs at 1064 nm.

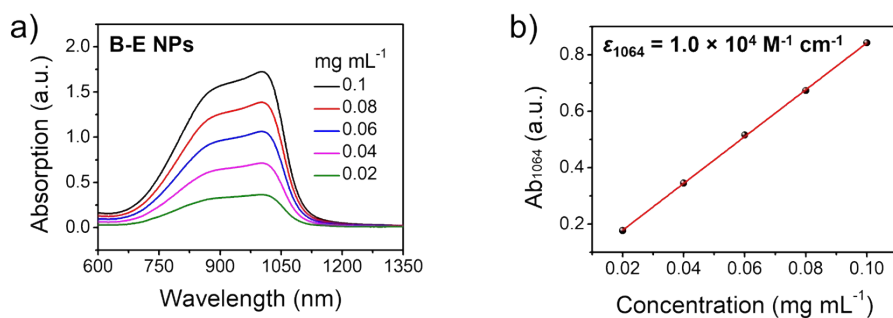


Fig. S23. (a) UV-vis-NIR spectra of B-E NPs in water at different concentration. (b)

The mole extinction coefficient of B-E NPs at 1064 nm.

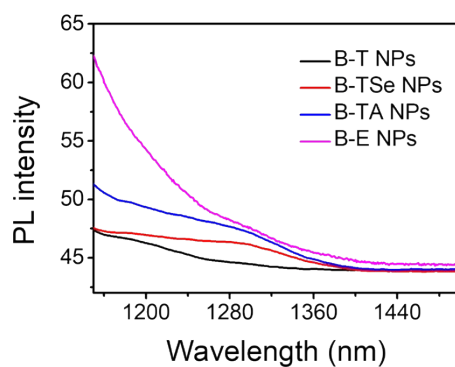


Fig. S24. The 1064 nm laser-excited emission spectra of B-Xs NPs in water at the same concentration.

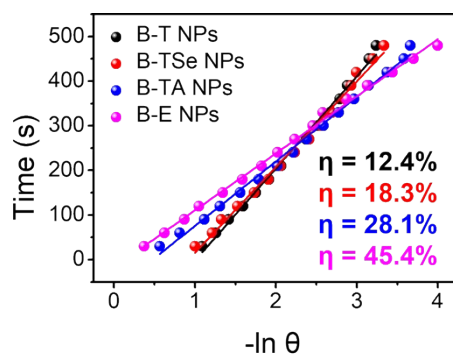


Fig. S25. NIR-II PCE calculations of B-Xs NPs under 1064-nm laser irradiation (1.0

W cm^{-2}) for 5 min. All the tests were performed at 100 μM .

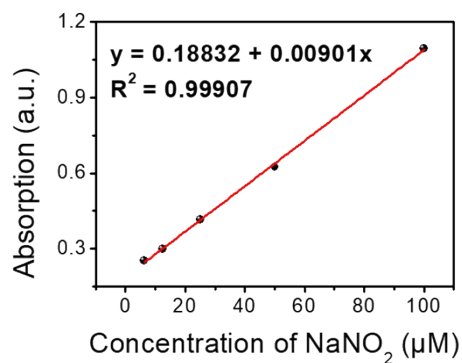


Fig. S26. The response curve of Griess agent to NO.

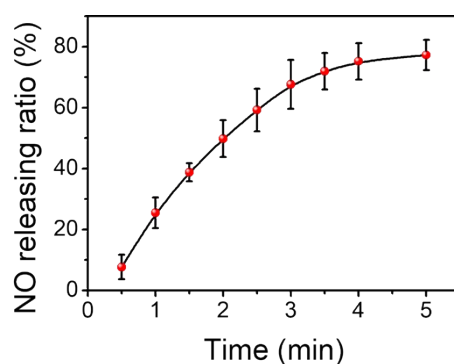


Fig. S27. The response curve of Griess agent to NO. The NO releasing ratio of B-E-NO NPs was calculated to be 77%, which shows a similar level to previous literature (*Biomaterials*, 2019, 217, 119304). This limited NO releasing ratio value could be attributed to the insufficient illumination time and rapid release of NO gas during the test, which failed to fully contact the probe.

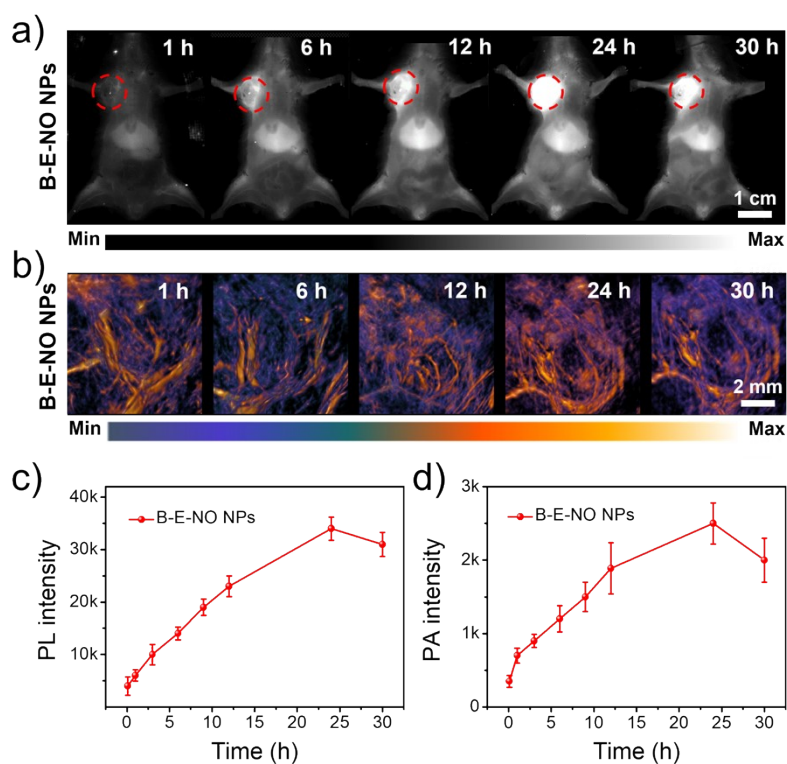


Fig. S28. *In vivo* (a) NIR-II FLI and (b) NIR-II PAI of B-E-NO NPs -treated 4T1 tumor-bearing mice under 1064 nm (the red dotted circles indicate the tumors). Corresponding quantification analysis of tumor (c) fluorescence intensity and (d) photoacoustic intensity at different monitoring times.

4. References

- [1] C. Xu, K. Pu, *Chem. Soc. Rev.* **2021**, *50*, 1111-1137.